

Activation of SIRT6 Deacetylation by DNA Strand Breaks

Published as part of ACS Omega virtual special issue "Nucleic Acids: A 70th Anniversary Celebration of DNA".

Wenjia Kang, Abu Hamza, Alyson M. Curry, Evan Korade, Dickson Donu, and Yana Cen*



Cite This: *ACS Omega* 2023, 8, 41310–41320



Read Online

ACCESS |



Metrics & More

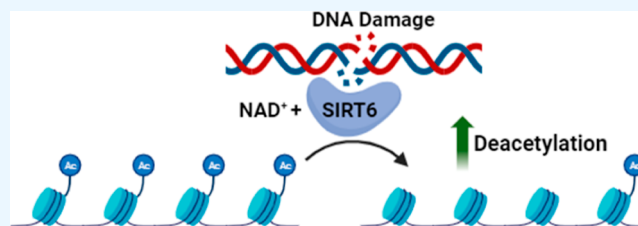


Article Recommendations



Supporting Information

ABSTRACT: SIRT6 is an emerging regulator of longevity. Overexpression of SIRT6 extends the lifespan of mice. Conversely, SIRT6 knockout mice demonstrate severe metabolic defects and a shortened lifespan. The discrepancy between SIRT6's weak *in vitro* activity and robust *in vivo* activity has led to the hypothesis that this enzyme can be activated in response to DNA damage in cells. Here, we demonstrate that the deacetylase activity of SIRT6 can be stimulated by DNA strand breaks for synthetic peptide and histone substrates. The mechanism of activation is further explored by using an integrative chemical biology approach. SIRT6 can be preferentially activated by DNA lesions harboring a 5'-phosphate. The N- and C-termini of SIRT6 are strictly required for DNA break-induced activation. Additionally, the defatty-acylase activity of SIRT6 is also sensitive to DNA breaks, although the physiological significance needs further investigation. Collectively, our study sheds important light on the cellular regulation of diverse SIRT6 activities and suggests possible strategies for effective SIRT6 activation.



INTRODUCTION

Sirtuins are a unique family of enzymes using NAD⁺ as a cosubstrate to remove the acetyl group from lysine residues. In addition to histone proteins, sirtuins also regulate other proteins and enzymes through their deacetylation activity. During calorie restriction (CR), several human sirtuins demonstrate elevated expression and activity.¹ This has been suggested to mediate the beneficial effect of CR, leading to an extended lifespan and improved health profiles in diverse organisms from archaea to human.¹ Thus, sirtuins have become novel therapeutic targets for the treatment of metabolic disorders and age-related diseases.

The current study focuses on one specific sirtuin isoform, SIRT6. SIRT6 is enriched in the nucleus and closely associated with chromatin.² The important role of SIRT6 in preventing genome instability and maintaining glucose and lipid homeostasis has been well-established.^{3–7} *Sirt6* null mice demonstrate a progeroid-like phenotype with metabolic defects and genome instability.^{3,6} In contrast, overexpression of *sirt6* in mice offers longevity benefits.^{8–10} Mounting evidence suggests that many of the cellular functions of SIRT6 are attributed to its NAD⁺-dependent deacetylase activity. Originally, SIRT6 was characterized as a histone deacetylase (HDAC) targeting specific sites on histone H3 (H3K9, H3K18, and H3K56).^{4,5,11} Removal of these histone marks by SIRT6 is important for chromatin condensation, transcription repression, and DNA damage response.¹² Notably, SIRT6 is a complex enzyme with substrates beyond histone lysines. It deacetylates several nonhistone proteins involved in DNA repair and glucose homeostasis.^{13,14}

The cellular activity of SIRT6 is highly regulated at multiple levels. At the transcriptional level, SIRT6 can be controlled by nuclear respiratory factor-1 (NRF-1), a transcription factor, in a hepatic-specific manner.¹⁵ Upon nutrient deprivation, NRF-1 interacts with the SIRT1/FOXO3a complex to induce SIRT6 transcription.¹⁵ At the post-translational level, CR or fasting leads to increased SIRT6 protein stability,¹⁶ which subsequently improves metabolic profiles in response to nutrient availability. Additionally, nitration of a tyrosine residue by peroxynitrite results in the reduction of SIRT6 enzymatic activity, although the exact mechanism of this inhibition is still not clear.¹⁷ Furthermore, SIRT6 activity is sensitive to the cellular NAD⁺ concentrations. Inhibition of nicotinamide phosphoribosyltransferase (NAMPT), the rate-limiting enzyme of the salvage pathway for NAD⁺ biosynthesis, by small molecule FK866 caused significant reduction of intracellular NAD⁺ contents.¹⁸ NAD⁺ depletion led to decreased production of tumor necrosis factor (TNF), most likely due to the inhibition of SIRT6 activity.¹⁸ Current understanding of sirtuin regulation does not consider allostery as an important and effective strategy to control activity and dynamic adaptability of the enzyme. The study of SIRT6 biology has been hindered by the lack of knowledge of its direct cellular

Received: July 6, 2023

Accepted: October 5, 2023

Published: October 23, 2023



targets. The weak *in vitro* deacetylase activity of SIRT6 has created ample controversies on the identity of this enzyme and its physiological substrates.¹⁹ We propose, with strong preliminary data, that the deacetylase activity of SIRT6 can be stimulated by DNA strand breaks. The tight allosteric regulation emanating from direct SIRT6–DNA interactions could increase the affinity of SIRT6 for acetylated histone substrates. Truncation analysis suggests that the N- and C-terminal domains are responsible for DNA binding and activity stimulation. Furthermore, the defatty-acylase activity of SIRT6 can also be activated by DNA damage, highlighting that the diverse enzymatic functions of SIRT6 can be coordinately controlled by DNA strand breaks.

Allosteric activation not only represents a novel regulatory mechanism but also helps explain the robust cellular deacetylase activity of SIRT6. There are several overarching aspects that make this study innovative. First, allosteric activators of sirtuin have been intensely pursued during the last ten years with little success and with ample controversies.^{20–22} In-depth analysis of allosteric activation of SIRT6 by DNA breaks not only expands our knowledge of allosteric regulation of SIRT6 on the molecular level but also suggests possible strategies for effective SIRT6 activation. More broadly, the work on SIRT6 provides a basis for possible generality of allosteric regulation of sirtuin functions. In another vein, the potential of sirtuin activation as a tractable chemical genetic approach remains significant. It could help decipher the intricate cellular regulation loops between SIRT6 and other signal pathways. Ultimately, the new mechanistic insights gained in this study will have a transformative impact on the study of SIRT6 biology and related fields. It will lead to the creation of innovative chemical tools for sirtuin regulations, the development of new paradigms for SIRT6 functions, and the discovery of new endogenous targets of SIRT6.

METHODS AND MATERIALS

Reagents and Instruments. All reagents were purchased from Sigma or Fisher Scientific and were of the highest purity commercially available. HPLC was performed on a Dionex Ultimate 3000 HPLC system equipped with a diode array detector using a Macherey-Nagel C18 reverse-phase column. Fluorescence scanning was performed on a Biorad ChemiDoc MP imaging system.

Synthetic Peptides. Synthetic peptides H3K9Ac: ARTKQTAR(K-Ac)STGGKAPRKQLAS and H3K9Myr: ARTKQTAR(K-Myr)STGGKAPRKQLAS were synthesized and purified by GenScript. The peptides were purified by HPLC to a purity >95%.

DNA. DNAs used in the current study are listed below:

ssDNA: 5'-AGCACTGCCTCTGGCATCCCCGACTTC-3'

dsDNA: calf thymus DNA (Sigma)

circular plasmid: pSTBlue (Novagen)

fluorescent dsDNA:

5'-CAGATCTACCGAATCAGTCCGACGACGCATCTGCACTACGAGGATAC/Alexa532/-3'

3'-GTCTAGATGGCTTAGTCAGGCTGCTGCGTAGACGTGATGCTCCTATG-5'

Protein Expression and Purification. Plasmids of full-length SIRT1, SIRT2 (38–356), SIRT3 (102–399), and SIRT5 (34–302) were generous gifts from Lin at Cornell University. The proteins were expressed and purified as described before.^{23,24} SIRT6 was a gift from Cheryl Arrow-

smith (Addgene plasmid # 28271). The protein was expressed and purified as described before.²⁵ The identity of the protein was confirmed by tryptic digestion, followed by LC-MS/MS analysis performed at the Vermont Biomedical Research Network (VBRN) Proteomics Facility. Protein concentrations were determined by the Bradford assay.

Deacetylation Assay. K_m and k_{cat} of SIRT6 were measured for both NAD⁺ and synthetic peptide substrate. A typical reaction was performed in 100 mM phosphate buffer, pH 7.5, in a total volume of 50 μ L. For NAD⁺ parameter measurement, the reactions contained various concentrations of NAD⁺ and 2 mM H3K9Ac. For synthetic peptide substrate measurement, the reactions contained various concentrations of H3K9Ac and 2 mM NAD⁺. Reactions were initiated by the addition of 10 μ M of SIRT6 and were incubated at 37 °C for 2 h before being quenched by 8 μ L of 10% trifluoroacetic acid (TFA). The samples were then injected on an HPLC and resolved by a Macherey-Nagel Nucleosil C18 column. Substrate and product peptides were resolved using a gradient of 10–40% acetonitrile in 0.1% TFA. Chromatograms were analyzed at 215 nm. Reactions were quantified by integrating area of peaks corresponding to substrate and product peptides. Rates were plotted as a function of substrate concentration and best fits of points to the Michaelis–Menten equation were performed by KaleidaGraph.

DNA Activation Assay. Reactions were carried out in 100 mM phosphate buffer pH 7.5 containing 800 μ M NAD⁺, 1 mM H3K9Ac, in the presence or absence of DNA. The reactions were initiated by the addition of 10 μ M SIRT6 and were incubated at 37 °C for 2 h before being quenched by 8 μ L of 10% TFA. The samples were then injected on an HPLC fitted to a Macherey-Nagel Nucleosil C18 column. Acetylated and deacetylated peptides were resolved using a gradient of 10–40% acetonitrile in 0.1% TFA. Chromatograms were analyzed at 215 nm. Reactions were quantified by integrating area of peaks corresponding to acetylated and deacetylated peptides. Apparent activation was expressed as a percentage ratio of $k_{cat}(\text{act.}) * K_m(\text{unact.}) / [k_{cat}(\text{unact.}) * K_m(\text{act.})]$.

Labeling of SIRT6 with Probe A. The synthesis of probe A has been reported previously.²⁶ The labeling experiments contained 500 μ M NAD⁺, 25 μ M probe A, 10 μ M SIRT6, and increasing concentrations of dsDNA (0 to 400 ng/ μ L) in 100 mM phosphate buffer at pH 7.5. The samples were incubated at 37 °C for 10 min before being transferred to a clear bottom 96-well plate. The plate was placed on ice and irradiated at 365 nm at 4 °C for 1 h. Azide fluor 545, CuSO₄, tris(2-carboxyethyl)phosphine (TCEP), and tris[(1-benzyl-1H-1,2,3-triazol-4-yl)methyl]amine (TBTA) were then added to the samples to initiate the “click” reactions. The samples were gently agitated at 250 rpm for 30 min at room temperature before being resolved on a 10% SDS-PAGE gel. The gel was destained in a mixture of methanol/distilled water/acetic acid (v/v/v = 4:5:1) for 4 h at room temperature. Subsequently, in-gel fluorescence analysis was performed using a Biorad ChemiDoc MP imager (excitation at 532 nm, 580 nm cutoff filter with a 30 nm band-pass). Coomassie staining was used as a loading control.

Electrophoretic Mobility Shift Assay. The dsDNA carrying a 3'-fluorophore was incubated with varying concentrations of SIRT6 (0 to 45 μ M) in DNA-binding buffer (20 mM Tris-HCl, pH 7.5, 150 mM NaCl, 5% glycerol). The samples were incubated on ice for 20 min. The samples were then resolved on a native 10% TBE gel at 4 °C. Visualization

and quantification of the gels were carried out using a Biorad ChemiDoc MP imaging system and Image Lab software. Any species migrating at a slower electrophoretic rate than free DNA were considered as a DNA–protein complex. Relative complex formation was plotted as a function of protein concentration and fitted to the equation: $f = f_{\max} [\text{SIRT6}]^h / (K_d + [\text{SIRT6}]^h)$, where f is the fractional saturation, f_{\max} is maximum complex formation, $[\text{SIRT6}]$ is the protein concentration, h is the Hill slope, and K_d reflects the binding affinity of the proteins to the DNA construct.

Histone Deacetylation Assay. A typical reaction was performed in 100 mM phosphate buffer pH 7.5 containing protease inhibitors, 500 μM NAD^+ , and 0.6 μg of calf thymus histone (Sigma), with or without 1.2 $\mu\text{g}/\mu\text{L}$ calf thymus DNA. The reaction was initiated with the addition of 10 μM SIRT6 and incubated at 37 $^\circ\text{C}$. At 0, 30, 60, and 120 min time points, aliquots were removed from the reaction and quenched by the addition of 4x Laemmli loading buffer. The samples were boiled at 95 $^\circ\text{C}$ for 10 min, resolved on a 10% SDS-PAGE, and analyzed by western blot.

Cell Culture. HEK293 and HeLa cells were cultured in DMEM supplemented with 10% fetal bovine serum, 100 U/mL penicillin, and 100 mg/mL streptomycin. Cells were maintained in a humidified 37 $^\circ\text{C}$ incubator with 5% CO_2 .

Metabolic Labeling. Cells were treated with either 20 μM azido myristic acid or DMSO (vehicle control) for 18 h. Cells were harvested, resuspended in PBS, and pelleted at 1000g for 5 min at 4 $^\circ\text{C}$. The cell pellet was then dissolved in RIPA buffer (Thermo Scientific) with Halt protease phosphatase inhibitor cocktail (Thermo Scientific). The lysate was centrifuged at 15,000g for 5 min at 4 $^\circ\text{C}$. The supernatant was used for the defatty-acylation analysis.

Defatty-Acylation Assay. Cell lysate was incubated with 500 μM NAD^+ , 10 μM SIRT6 with or without calf thymus DNA at 37 $^\circ\text{C}$ for 1 h. The samples were then incubated with 15 mM iodoacetamide at room temperature for 30 min before the addition of TAMRA-DBCO. The samples were incubated at room temperature for another 30 min. Subsequently, the samples were heated with NH_2OH (60 mM, pH 7.2) at 95 $^\circ\text{C}$ for 7 min before being resolved by SDS-PAGE. The destained gel was analyzed with in-gel fluorescence scanning using a Biorad ChemiDoc MP imager (excitation at 532 nm, 580 nm cutoff filter, and 30 nm band-pass).

Western Blot. The samples were resolved on a 10% SDS-PAGE gel and transferred to an Immobilon PVDF transfer membrane (Biorad). The blot was blocked with 5% nonfat milk, probed with primary antibody, washed with TBST, followed by incubation with antirabbit HRP-conjugated secondary antibody. The signal was then detected by Clarity western ECL substrate (Biorad).

RESULTS AND DISCUSSION

SIRT6 Deacetylation can be Stimulated by DNA Strand Breaks. We have expressed full-length human SIRT6 with an N-terminal His-tag. It has the ability to deacetylate a short peptide sequence that is identical to the N-terminus of histone H3 bearing the acetylated lysine 9 mark (H3K9Ac, Figure 1A). The recombinant enzyme is also able to deacetylate H3K9Ac in acid precipitated whole histone (Figure 1B).⁴ The kinetic constants for SIRT6-mediated deacetylation under steady state conditions at pH 7.5 were determined (Table 1). The Michaelis–Menten constants of SIRT6 for H3K9Ac and NAD^+ are 1670 ± 115 and 150 ± 21 μM ,

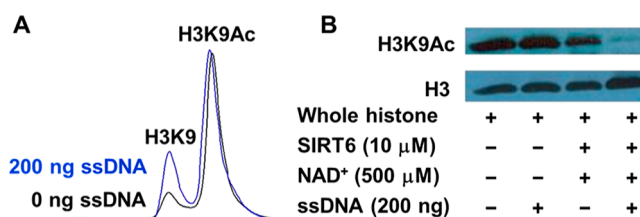


Figure 1. SIRT6 deacetylation activity is activated by ssDNA. (A) Overlay of HPLC chromatograms of SIRT6-catalyzed deacetylation of H3K9Ac peptide with or without DNA; and (B) western blot of SIRT6-catalyzed deacetylation of whole histone with or without DNA.

Table 1. Recombinant SIRT6 Steady State Parameters

substrate	additive	K_m (μM)	k_{cat} (10^{-3} s^{-1})	M.A. ^c
H3K9Ac ^a		1670 ± 115	1.5 ± 0.2	1.0
H3K9Ac	ssDNA ^c	520 ± 84	2.1 ± 0.6	4.4
H3K9Ac	dsDNA ^d	470 ± 55	2.0 ± 0.4	4.6
NAD^{+b}		150 ± 21	0.84 ± 0.2	1.0
NAD^+	ssDNA	290 ± 23	1.4 ± 0.3	0.86
NAD^+	dsDNA	200 ± 28	1.8 ± 0.4	1.50

^aAt 2 mM NAD^+ . ^bAt 2 mM H3K9Ac. ^c $[\text{ssDNA}] = 100 \text{ ng}/\mu\text{L}$, sequence: 5'-AGCACTGCCTCTGGCATCCCCGACTTC-3'. ^d $[\text{dsDNA}] = 300 \text{ ng}/\mu\text{L}$. ^eM.A.: Maximal Activation = $k_m(\text{act.}) * K_m(\text{unact.}) / [k_m(\text{unact.}) * K_m(\text{act.})]$.

respectively. In *in vitro* testing, SIRT6 demonstrated low affinity toward synthetic peptide substrates, consistent with the previous reports.^{19,27}

Recently, SIRT6 has been found to be a DNA-binding protein.^{7,28,29} Our own results confirmed this (Figure 2): in all

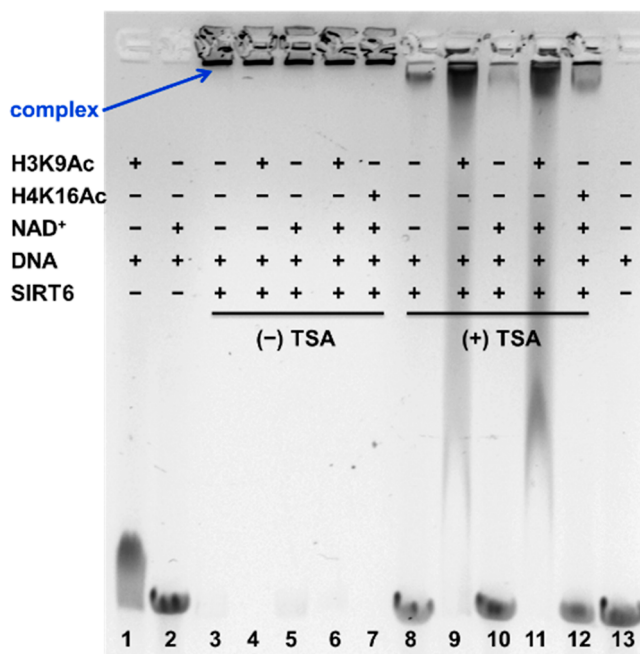


Figure 2. SIRT6 is a DNA-binding protein. Linearized pSTBlue plasmid was incubated with the ingredients indicated in the image and resolved on a 0.6% native agarose gel stained with ethidium bromide. Addition of recombinant SIRT6 (lanes 3 to 7) led to the formation of a SIRT6–DNA complex (blue arrow) that stayed in the well. Addition of TSA, a recently discovered SIRT6 inhibitor, was able to dissociate the complex (lanes 8 to 12).

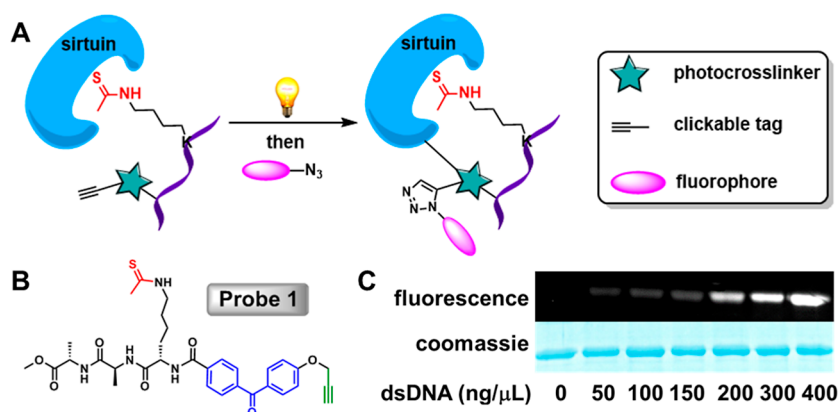


Figure 3. Detection of DNA-induced SIRT6 activation by an activity-based chemical probe. (A) General scheme of the labeling protocol; (B) chemical structure of probe 1; and (C) DNA-induced labeling of SIRT6 by probe 1. Mixtures of human SIRT6, NAD^+ , and probe 1 were incubated with indicated concentrations of dsDNA. The samples were photo-cross-linked and “click”-conjugated to a fluorophore before being resolved on a SDS-PAGE gel.

the samples containing both recombinant SIRT6 and linearized pSTBlue plasmid (lanes 3 to 7), the formation of a stable SIRT6–DNA complex can be easily detected (indicated by the blue arrow). The addition of peptide substrate and/or NAD^+ caused negligible changes (lanes 4 to 7 vs lane 3). Interestingly, the protein–DNA complex was disrupted by the introduction of trichostatin A (TSA, lanes 8 to 12). We recently discovered that TSA selectively inhibits SIRT6 among all the human sirtuins with the IC_{50} in the low micromolar range.²⁷ This result suggests that TSA and DNA may compete, at least partially, for the same binding site. These initial findings, together with several recent reports showing that SIRT6 demonstrates a nucleosome-dependent deacetylase activity,^{28,30–32} prompted us to investigate whether the deacetylation activity of SIRT6 can be stimulated by DNA as part of its normal function. Indeed, when DNA [ssDNA, dsDNA (calf thymus DNA sheared to an average size less than 2000bp), or cut plasmid] was included in the reaction, SIRT6 deacetylation was significantly improved toward the peptide substrate (Figure 1A and Table 1). This activation is selective for SIRT6 because DNA failed to activate human SIRT1, SIRT2, SIRT3, or SIRT5 to any appreciable levels (Figure S1). Similar activation effect was also observed in the deacetylation of whole histone by SIRT6 (Figure 1B). Strikingly, intact circular plasmids and RNAs (Figure S2) failed to elicit such a response, suggesting that this activation is specific to DNA breaks. We further characterized this activation by steady state kinetics analysis (Table 1). The addition of ssDNA or dsDNA caused a significant reduction of K_m of SIRT6 to H3K9Ac (Table 1, rows 3 and 4). This activation is saturable, indicating a distinct binding site for DNA (Figure S3).

Activity-based chemical probes (ABPs) have been developed by us for the evaluation of active sirtuin components in their native matrix.²⁶ These probes are tripeptides carrying a thioacyl “warhead” on the lysine residue, a photoactivatable group for the covalent tethering of the probe to the enzyme target, and a terminal alkyne for the “click” conjugation to a fluorophore. The schematic representation of a typical labeling experiment is shown in Figure 3A. ABP labeling assay was used to sensitively detect DNA-induced SIRT6 activation. One of the probes, probe 1 (Figure 3B), showed negligible labeling of human SIRT6 without DNA. However, the introduction of dsDNA to the reaction mixture resulted in a concentration-

dependent labeling of SIRT6 by probe 1 (Figure 3C). This analysis yielded an activation constant (EC_{50}) of 157 $\text{ng}/\mu\text{L}$ for dsDNA. Notably, this value is in good agreement with the EC_{50} determined by the HPLC assay, which is 122 $\text{ng}/\mu\text{L}$.

It is important to note that several recent studies demonstrate that SIRT6 has intrinsic affinity to nucleosomes (undamaged DNA).^{28,31,32} Our results, however, suggest that SIRT6 can also be activated by DNA lesions. It is known that SIRT6 can be quickly (within 5 s) recruited to DNA damage sites in response to oxidative stress.^{33–35} Subsequently, SIRT6 participates in DNA repair through either direct deacetylation of damaged-DNA-binding protein 2 (DDB2),¹⁴ the recruitment and stimulation of PARP-1,³⁴ or serving as a double-strand breaks (DSBs) sensor.^{7,29} Rapid loss of H3K9Ac and H3K56Ac has been observed as a global response to DNA damage.³⁶ Our preliminary data strongly suggest that SIRT6 is activated following recognition of DNA breaks, and this heightened deacetylation activity will further facilitate DNA damage repair.

DNA Binding Preference of SIRT6. Given that DNA breaks are crucial for enzyme activation, we asked if SIRT6 could recognize different DNA interruptions independent of the sequence. As shown in our preliminary data, the stimulation of SIRT6 deacetylase activity is dependent on single- or double-stranded DNA interruptions (Figures 1, 3, and S3). Closed circular DNA is ineffective as an activator unless it is linearized by restriction enzymes (Figure 4, uncut pSTBlue vs *Bam*HI or *Eco*RV treated), which is in good agreement with a previous notion that SIRT6 does not bind to circular plasmids.⁷ Strand breaks with overhangs are preferred over blunt ends (*Bam*HI treated vs *Eco*RV treated). 5'-Phosphate ends are more efficient activators than dephosphorylated termini (Figure 4, CIP treated vs untreated).

The preference to sticky ends and 5'-phosphorylated breaks may have interesting implications for SIRT6's involvement in DNA damage repair. SIRT6 has been shown to be a crucial first-line sensor of DSBs.^{7,33} Subsequently, it recruits SNF2H, a chromatin remodeler, to the damage site.³⁵ SIRT6 promotes classical nonhomologous end joining (NHEJ) by stabilizing NHEJ and homologous recombination (HR) by activating PARP-1.^{34,38} Despite the diversity of DNA lesions, the recruitment of SIRT6 to the damage site and the subsequent

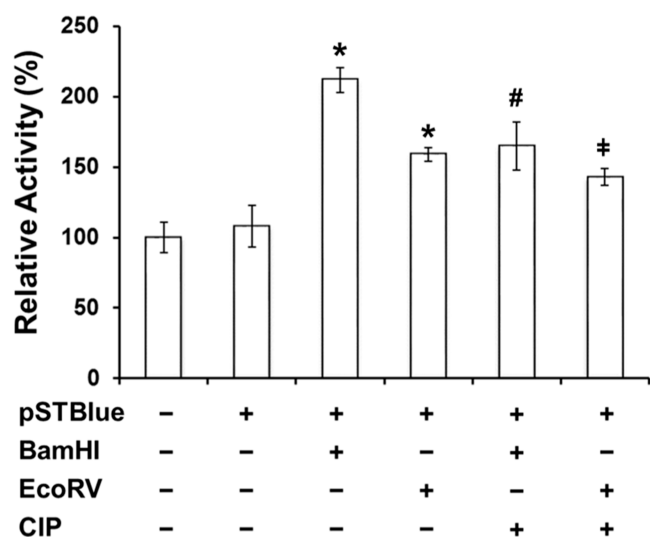


Figure 4. SIRT6 deacetylation can be stimulated by a linearized plasmid. SIRT6, NAD⁺, and H3K9Ac peptide were incubated in the presence of various forms of DNA including uncut pSTBlue plasmid, pSTBlue digested with *Bam*HI, pSTBlue digested with *Eco*RV, *Bam*HI digested, and CIP (calf intestinal alkaline phosphatase) treated pSTBlue, or *Eco*RV digested and CIP treated pSTBlue. The final concentration of DNA is 50 ng/μL. The samples were analyzed as described in “Methods and Materials”. The quantification data represents average of three independent experiments ± SD. Statistical significance was determined by a Student’s *t*-test: **p* < 0.05 vs no DNA control; #*p* < 0.05 vs *Bam*HI-digested pSTBlue; ‡*p* < 0.05 vs *Eco*RV-digested pSTBlue.

SIRT6-mediated signaling must be fast and robust to maintain the dynamic range and tight regulation required for SIRT6’s cellular functions. Our results suggest that overhangs and 5′-phosphorylated DNAs lead to an elevated level of SIRT6-catalyzed deacetylation that could in turn signal the presence

of unsealed breaks and enhance the recruitment of repair enzymes.

N- and C-Terminal Regions of SIRT6 Are Required for DNA Break-Dependent Activation. The domain(s) responsible for DNA-induced activation was further investigated. The *sirt6* gene encodes a protein of 355 amino acid (AA) residues. The N-terminus of SIRT6 is indispensable for its enzymatic activity and association with chromatin, while the C-terminus is imperative for its subcellular localization.² Our initial effort focused on the N-terminus because of its importance in the chromatin interaction. We have constructed a series of truncations of SIRT6 by the sequential removal of blocks of AAs from the N-terminal end (Figure 5A). HPLC assay using synthetic H3K9Ac peptide and western blot using whole histone as the substrate were used to assess the activity of these truncated SIRT6s (Figure 5B,C). For comparison, the SIRT6H133Y protein, a catalytically inactive SIRT6 mutant, was also included in the study. Consistent with a previous report,² removal of the entire N-terminus (ΔN) completely abrogated the ability of SIRT6 to reduce H3K9 acetylation, similar to the H133Y mutant. Intriguingly, deletion of the first 12 AAs did not cause any significant reduction of the SIRT6 deacetylation activity. However, the DNA activation effect was severely compromised in this truncation, suggesting the critical role of this region in mediating DNA-induced SIRT6 activation. Moreover, this result is consistent with bioinformatics analysis using DP-Bind^{39,40} predicting that the N- (4-12) are potential DNA-binding sites (Figure S4).

The C-terminal domain has been suggested as a DNA-binding domain that is responsible for the interaction of SIRT6 with the nucleosome at a high affinity binding site.²⁸ We set out to evaluate if this region is essential for the binding to DNA strand breaks through truncation analysis. Several C-terminal truncates including SIRT6(1–280), SIRT6(1–300), SIRT6(1–320), and SIRT6(1–340) were expressed and purified (Figure S5A). The identity of the truncates was

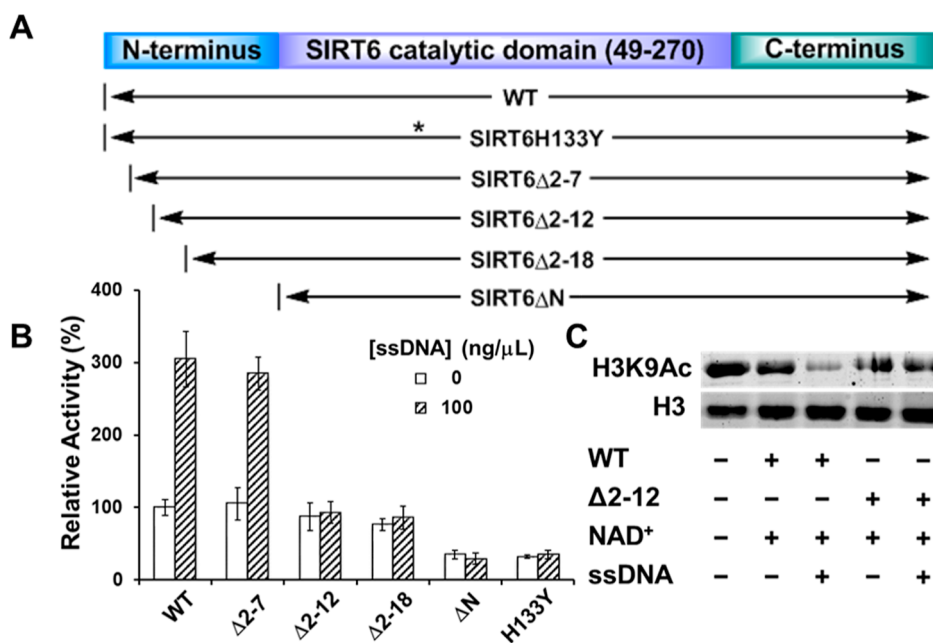


Figure 5. N-terminus of SIRT6 is important for its activation by DNA. (A) Schematic representation of the SIRT6 deletions and point mutant; (B) relative deacetylation activity of SIRT6 with or without ssDNA as determined by the HPLC assay; and (C) a representative western blot showed SIRT6 activity on the histone substrate.

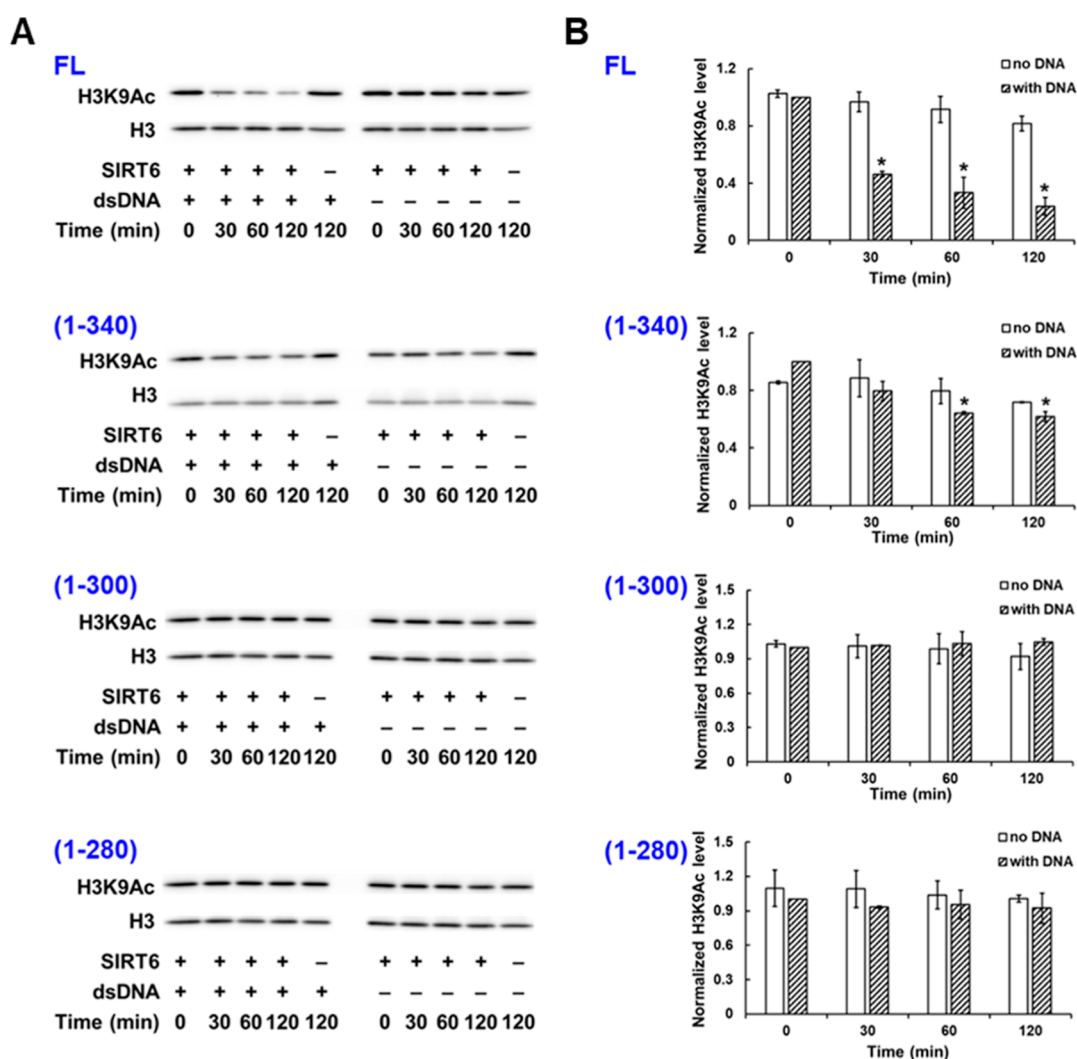


Figure 6. Importance of the C-terminus of SIRT6 for its activation by dsDNA. (A) Representative western blots showing the deacetylase activity of different C-terminal truncates of SIRT6 on histone substrate in the presence or absence of dsDNA; (B) quantification of the western blot results in (A). The H3K9Ac level was normalized by the amount of histone H3 protein. The relative H3K9Ac level was calculated by setting the level of no enzyme control to 100%. The quantification data represents average of three independent experiments \pm SD. Statistical significance was determined by a Student's *t*-test: * $p < 0.05$ vs no DNA control.

further confirmed by tryptic digestion coupled to proteomics analysis. The steady state parameters of these truncated samples were also determined using the HPLC assay described in “Methods and Materials”. SIRT6(1–280) demonstrated significantly decreased catalytic efficiency, while the other three truncates were comparable to the full-length protein (Figure S5B). Similar results were obtained using calf thymus histone as the substrate (Figure 6). In the presence of dsDNA, the acetylation level of H3K9 was markedly reduced by SIRT6FL compared to that of the no DNA controls. SIRT6(1–280), in contrast, lacked appreciable enzymatic activity and was inert to DNA activation, consistent with the HPLC results. Interestingly, the deacetylase activity of SIRT6(1–340) could also be stimulated by dsDNA, albeit to a lesser extent. In addition, removal of the last 55 AAs [truncate SIRT6(1–300)] completely abolished the DNA activation effect, further highlighting the importance of the C-terminal domain in mediating DNA strand break-induced SIRT6 activation.

The ability of the C-terminal variants to bind to DNA breaks was evaluated using the electrophoretic mobility shift assay (EMSA) with a duplex oligodeoxynucleotide (ODN) carrying

a 3'-fluorophore (Figure 7A). Figure 7B illustrates the representative gel images and binding curves of SIRT6 as determined by EMSA. SIRT6FL demonstrated tight binding to dsDNA with a K_D value of $1.93 \pm 0.10 \mu\text{M}$ (Figure 7C). The binding was significantly attenuated with the removal of C-terminal AAs: the K_D value of SIRT6(1–300) was determined to be $9.68 \pm 0.39 \mu\text{M}$, 5 times higher than that of the full-length enzyme. Interestingly, SIRT6 exhibited cooperative binding effect to the dsDNA with Hill coefficient greater than 1, which is in good agreement with a recent report.⁷ Taken together, the C-terminus of SIRT6 is strictly required for DNA break binding and subsequent activity stimulation.

Several structural biology studies suggest that the C-terminal extension of SIRT6 is highly unstructured,^{28,31,41} as predicted by AlphaFold (Figure S6).^{42,43} One intriguing model is that the binding of SIRT6 to DNA lesion is primarily regulated by the N- and C-terminal extensions. Upon binding to DNA damage, these intrinsically disordered regions^{31,41} become organized to induce a conformational change to activate SIRT6. This fascinating phenomenon warrants further investigation.

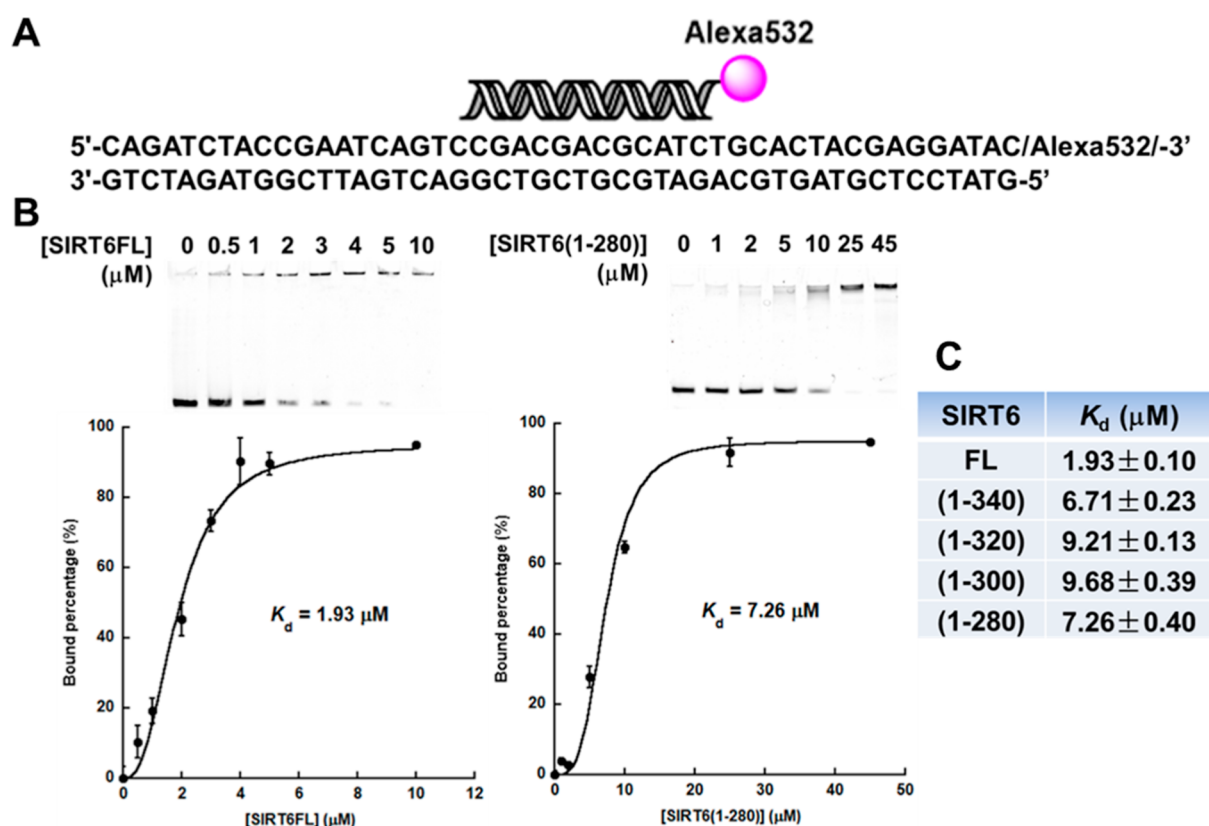


Figure 7. C-terminal domain of SIRT6 is critical for DNA binding. (A) Schematic representation of the fluorescent ODN used in the EMSA. The sequence of the dsDNA is listed below; (B) EMSA. Top: representative gel images of SIRT6FL and SIRT6(1-280); bottom: binding affinity analysis; and (C) binding affinity of SIRT6 truncates determined by EMSA.

It is important to point out that the binding of two SIRT6s to one nucleosome core particle with differential affinities has been proposed.²⁸ The high affinity binding complex was solved by cryo-EM structural analysis^{31,32} and has been suggested to be responsible for the substrate preference of SIRT6. The model proposed in this study could represent the low affinity binding poise: SIRT6 is able to move along undamaged DNA, use the N- and C-termini to scan and bind to ruptured DNA strands, and then recruit other repair enzymes to the damage site.

DNA Activates SIRT6-Catalyzed Defatty-Acylation.

Recent studies suggest that in addition to the deacetylation activity, SIRT6 also possesses defatty-acylase activity. It prefers to hydrolyze long chain fatty acyl groups from lysine residues.^{19,44} Through this novel modification, SIRT6 promotes the secretion of TNF- α ¹⁹ and also regulates the membrane localization of R-Ras2.⁴⁵ As SIRT6 is poised at the intersection between chromatin modulation, metabolism, and genome maintenance, understanding how SIRT6 regulates this novel activity is highly intriguing. Using a myristoylated synthetic H3K9 peptide (H3K9Myr) as the substrate, we characterized the defatty-acylase activity of wtSIRT6 (Figure S7). The catalytic efficiency (k_{cat}/K_m) of demyristoylation was 250-fold higher than that of the deacetylation ($227.8 \text{ M}^{-1} \text{ s}^{-1}$ vs $0.9 \text{ M}^{-1} \text{ s}^{-1}$), further confirming the robust *in vitro* defatty-acylase activity of SIRT6.

Detection of defatty-acylation of cellular proteins was performed by metabolic labeling with azido myristic acid (Az-myristic).⁴⁶ HEK293 cells were cultured in the presence of Az-myristic which covalently labels cellular protein targets (Figure

8A). The whole cell lysate was treated with wtSIRT6 in the presence or absence of dsDNA. The labeled proteins were then conjugated to TAMRA-DBCO *via* the copper-free “click” reaction. Since Az-myristic also acylates Cys residues, the samples were further treated with NH_2OH to remove S-acylation. Finally, the labeled lysate was resolved by SDS-PAGE and analyzed by in-gel fluorescence scanning (Figure 8B). Az-myristic treated cell lysate exhibited significantly increased labeling compared to the control cell lysate. Incubation of the lysate with wtSIRT6 markedly reduced the labeling intensity of numerous proteins, consistent with the notion that SIRT6 regulates the fatty acylation of endogenous protein targets.¹⁹ Furthermore, the introduction of dsDNA caused an additional reduction of the fluorescence signal of several proteins. To our knowledge, this represents the first example of the regulation of SIRT6 defatty-acylase activity by DNA strand breaks. The physiological relevance of this regulatory mechanism is being pursued in our laboratory.

CONCLUSIONS AND PERSPECTIVES

Studies from the past decade revealed that SIRT6 is a complex enzyme with diverse catalytic activities. In addition to deacetylation and mono-ADP-ribosylation, SIRT6 also harbors defatty-acylation activity.^{19,44} These pleiotropic enzymatic activities give SIRT6 its far-reaching functions in maintaining genome integrity^{47,48} and energy homeostasis.^{45,49} The important biological roles of SIRT6 influence cardiovascular disease,⁵⁰ diabetes,⁵¹ inflammation,⁵² and cancer,^{52,53} thereby impacting healthy organismal aging. The robust cellular deacetylase activity of SIRT6^{4,47,49,54} cannot be explained by

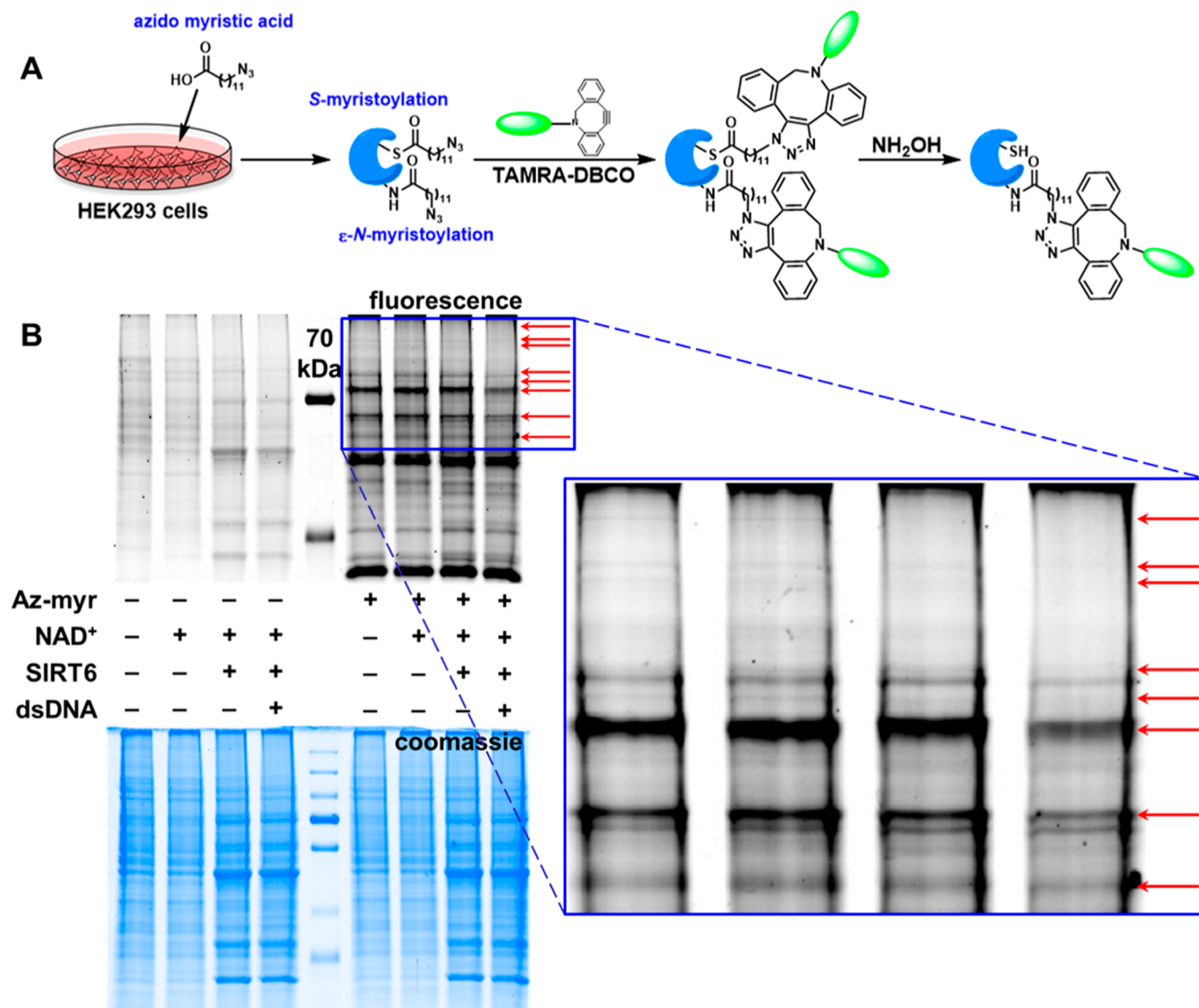


Figure 8. Defatty-acylase activity of SIRT6 can be activated by dsDNA. (A) Schematic representation of the labeling protocol; (B) defatty-acylation of cellular proteins by SIRT6. The lysate from Az-myristoylated cells showed increased labeling compared to the control cells. Incubation of the lysate with SIRT6 in the presence of dsDNA reduced the labeling intensity of several proteins compared to the no DNA control. Arrows highlight proteins with decreased fluorescence due to dsDNA exposure.

the weak *in vitro* data or the defatty-acylase activity. This discrepancy has led to the hypothesis that SIRT6 activity can be upregulated by endogenous allosteric activators, such as DNA strand breaks. Current understanding of sirtuin catalytic function and regulation within the cells fails to consider allostery as important. The need to dissect the allosteric activation of SIRT6 on the molecular level becomes apparent.

In this study, we complemented classical enzyme kinetics analysis with novel biochemical assays to interrogate the allosteric regulation of SIRT6 by DNA strand breaks. When synthetic peptides or whole histone was used as the substrate, the deacetylase activity of SIRT6 could be stimulated by ssDNA and dsDNA to similar extents. Although SIRT6's involvement in the cellular response to DNA damage is well-established, our results represent the first direct evidence that the enzymatic function of SIRT6 can be stimulated upon binding to DNA lesions. Subsequently, the DNA-binding preference was evaluated. Using a panel of DNAs mimicking naturally occurring DNA damage and repair intermediates, it

was determined that duplexes with overhangs were preferred over blunt ends; phosphorylated ends were more efficient activators than the dephosphorylated termini. To map the binding regions and provide residue-level insight into how SIRT6 associates with DNA breaks, we introduced truncations of varying lengths at the N- and C-terminal regions. Removal of the first 12 AAs from the N-terminus almost completely abolished the DNA activation effect without compromising the deacetylase activity. Similarly, the C-terminal truncate missing the last 55 AAs showed comparable deacetylase activity to the full-length protein but was inert to DNA break-induced activation stemming from a reduced binding affinity as evidenced by EMSA studies. A model consistent with the aforementioned data involved the searching and binding to DNA lesions of SIRT6 by both the N- and C-termini, followed by a structural rearrangement for elevated deacetylase activity. Moreover, the defatty-acylation of SIRT6 was also sensitive to DNA breaks. When challenged with DNA damage mimics, SIRT6-mediated defatty-acylation of cellular proteins could be

significantly increased, suggesting the multiple roles of DNA breaks in regulating SIRT6 physiological functions.

One of the limitations of the current study is that it does not account for the effect of the cellular architecture on studied biochemical processes. SIRT6's interactions with chromatin in cells are affected by many other macromolecules, which can either strengthen or weaken the interactions across multiple microenvironments. Thus, it is important to test the significance of SIRT6 activation by DNA strand breaks in a more physiologically relevant setting. The temporal and spatial relationships of SIRT6 and DNA lesions are investigated using cellular and biophysical approaches. All of these can be expected from our laboratory in the near future.

Overall, the studies presented here provide many details about the DNA damage recognition and activation of SIRT6 at the molecular level. They also help reconcile the early concerns about the discordant *in vitro* and *in vivo* deacetylase activities. The knowledge gained in these studies warrants the elucidation of new regulation strategies of SIRT6, which will facilitate the discovery of direct cellular targets of this enzyme.

■ ASSOCIATED CONTENT

SI Supporting Information

The Supporting Information is available free of charge at <https://pubs.acs.org/doi/10.1021/acsomega.3c04859>.

Design and cloning of SIRT6 truncates, expression and purification of SIRT6 truncates, and digestion of pSTBlue (PDF)

■ AUTHOR INFORMATION

Corresponding Author

Yana Cen – Department of Medicinal Chemistry, Virginia Commonwealth University, Richmond, Virginia 23298-0540, United States; Institute for Structural Biology, Drug Discovery and Development, Virginia Commonwealth University, Richmond, Virginia 23298-0133, United States; orcid.org/0000-0001-6436-5744; Phone: 804-828-7405; Email: ceny2@vcu.edu

Authors

Wenjia Kang – Department of Medicinal Chemistry, Virginia Commonwealth University, Richmond, Virginia 23298-0540, United States

Abu Hamza – Department of Medicinal Chemistry, Virginia Commonwealth University, Richmond, Virginia 23298-0540, United States

Alyson M. Curry – Department of Medicinal Chemistry, Virginia Commonwealth University, Richmond, Virginia 23298-0540, United States

Evan Korade – Department of Medicinal Chemistry, Virginia Commonwealth University, Richmond, Virginia 23298-0540, United States

Dickson Donu – Department of Medicinal Chemistry, Virginia Commonwealth University, Richmond, Virginia 23298-0540, United States

Complete contact information is available at:

<https://pubs.acs.org/doi/10.1021/acsomega.3c04859>

Notes

The authors declare no competing financial interest.

■ ACKNOWLEDGMENTS

This work was supported in part by CHE-1846785 from NSF (to Y.C.). MS analysis reported in this manuscript was performed at the Vermont Biomedical Research Network (VBRN) proteomics facility supported by P20GM103449 (NIH/NIGMS).

■ REFERENCES

- (1) Guarente, L. Calorie restriction and sirtuins revisited. *Genes Dev.* **2013**, *27* (19), 2072–2085.
- (2) Tennen, R. I.; Berber, E.; Chua, K. F. Functional dissection of SIRT6: identification of domains that regulate histone deacetylase activity and chromatin localization. *Mech. Ageing Dev.* **2010**, *131* (3), 185–192.
- (3) Xiao, C.; Kim, H. S.; Lahusen, T.; Wang, R. H.; Xu, X.; Gavrilova, O.; Jou, W.; Gius, D.; Deng, C. X. SIRT6 deficiency results in severe hypoglycemia by enhancing both basal and insulin-stimulated glucose uptake in mice. *J. Biol. Chem.* **2010**, *285* (47), 36776–36784.
- (4) Michishita, E.; McCord, R. A.; Berber, E.; Kioi, M.; Padilla-Nash, H.; Damian, M.; Cheung, P.; Kusumoto, R.; Kawahara, T. L.; Barrett, J. C.; Chang, H. Y.; Bohr, V. A.; Ried, T.; Gozani, O.; Chua, K. F. SIRT6 is a histone H3 lysine 9 deacetylase that modulates telomeric chromatin. *Nature* **2008**, *452* (7186), 492–496.
- (5) Michishita, E.; McCord, R. A.; Boxer, L. D.; Barber, M. F.; Hong, T.; Gozani, O.; Chua, K. F. Cell cycle-dependent deacetylation of telomeric histone H3 lysine K56 by human SIRT6. *Cell Cycle* **2009**, *8* (16), 2664–2666.
- (6) Mostoslavsky, R.; Chua, K. F.; Lombard, D. B.; Pang, W. W.; Fischer, M. R.; Gellon, L.; Liu, P.; Mostoslavsky, G.; Franco, S.; Murphy, M. M.; Mills, K. D.; Patel, P.; Hsu, J. T.; Hong, A. L.; Ford, E.; Cheng, H. L.; Kennedy, C.; Nunez, N.; Bronson, R.; Frendewey, D.; Auerbach, W.; Valenzuela, D.; Karow, M.; Hottiger, M. O.; Hursting, S.; Barrett, J. C.; Guarente, L.; Mulligan, R.; Dipple, B.; Yancopoulos, G. D.; Alt, F. W. Genomic instability and aging-like phenotype in the absence of mammalian SIRT6. *Cell* **2006**, *124* (2), 315–329.
- (7) Onn, L.; Portillo, M.; Ilic, S.; Cleitman, G.; Stein, D.; Kaluski, S.; Shirat, I.; Slobodnik, Z.; Einav, M.; Erdel, F.; Akabayov, B.; Toiber, D. SIRT6 is a DNA double-strand break sensor. *Elife* **2020**, *9*, No. e51636.
- (8) Kanfi, Y.; Naiman, S.; Amir, G.; Peshti, V.; Zinman, G.; Nahum, L.; Bar-Joseph, Z.; Cohen, H. Y. The sirtuin SIRT6 regulates lifespan in male mice. *Nature* **2012**, *483* (7388), 218–221.
- (9) Roichman, A.; Kanfi, Y.; Glazz, R.; Naiman, S.; Amit, U.; Landa, N.; Tinman, S.; Stein, I.; Pikarsky, E.; Leor, J.; Cohen, H. Y. SIRT6 Overexpression Improves Various Aspects of Mouse Healthspan. *J. Gerontol A Biol. Sci. Med. Sci.* **2017**, *72* (5), 603–615.
- (10) Roichman, A.; Elhanati, S.; Aon, M. A.; Abramovich, I.; Di Francesco, A.; Shahar, Y.; Avivi, M. Y.; Shurgi, M.; Rubinstein, A.; Wiesner, Y.; Shuchami, A.; Petrover, Z.; Leberthal-Loinger, I.; Yaron, O.; Lyashkov, A.; Ubaida-Mohien, C.; Kanfi, Y.; Lerrer, B.; Fernandez-Marcos, P. J.; Serrano, M.; Gottlieb, E.; de Cabo, R.; Cohen, H. Y. Restoration of energy homeostasis by SIRT6 extends healthy lifespan. *Nat. Commun.* **2021**, *12* (1), 3208.
- (11) Tasselli, L.; Xi, Y.; Zheng, W.; Tennen, R. I.; Odrowaz, Z.; Simeoni, F.; Li, W.; Chua, K. F. SIRT6 deacetylates H3K18ac at pericentric chromatin to prevent mitotic errors and cellular senescence. *Nat. Struct. Mol. Biol.* **2016**, *23* (5), 434–440.
- (12) Chang, A. R.; Ferrer, C. M.; Mostoslavsky, R. SIRT6, a Mammalian Deacetylase with Multitasking Abilities. *Physiol Rev.* **2020**, *100* (1), 145–169.
- (13) Dominy, J. E., Jr.; Lee, Y.; Jedrychowski, M. P.; Chim, H.; Jurczak, M. J.; Camporez, J. P.; Ruan, H. B.; Feldman, J.; Pierce, K.; Mostoslavsky, R.; Denu, J. M.; Clish, C. B.; Yang, X.; Shulman, G. I.; Gygi, S. P.; Puigserver, P. The deacetylase Sirt6 activates the acetyltransferase GCN5 and suppresses hepatic gluconeogenesis. *Mol. Cell* **2012**, *48* (6), 900–913.

- (14) Geng, A.; Tang, H.; Huang, J.; Qian, Z.; Qin, N.; Yao, Y.; Xu, Z.; Chen, H.; Lan, L.; Xie, H.; Zhang, J.; Jiang, Y.; Mao, Z. The deacetylase SIRT6 promotes the repair of UV-induced DNA damage by targeting DDB2. *Nucleic Acids Res.* **2020**, *48* (16), 9181–9194.
- (15) Kim, H. S.; Xiao, C.; Wang, R. H.; Lahusen, T.; Xu, X.; Vassilopoulos, A.; Vazquez-Ortiz, G.; Jeong, W. I.; Park, O.; Ki, S. H.; Gao, B.; Deng, C. X. Hepatic-specific disruption of SIRT6 in mice results in fatty liver formation due to enhanced glycolysis and triglyceride synthesis. *Cell Metab.* **2010**, *12* (3), 224–236.
- (16) Kanfi, Y.; Shalman, R.; Peshiti, V.; Pilosof, S. N.; Gozlan, Y. M.; Pearson, K. J.; Lerrer, B.; Moazed, D.; Marine, J. C.; de Cabo, R.; Cohen, H. Y. Regulation of SIRT6 protein levels by nutrient availability. *FEBS Lett.* **2008**, *582* (5), 543–548.
- (17) Hu, S.; Liu, H.; Ha, Y.; Luo, X.; Motamedi, M.; Gupta, M. P.; Ma, J. X.; Tilton, R. G.; Zhang, W. Posttranslational modification of Sirt6 activity by peroxynitrite. *Free Radic Biol. Med.* **2015**, *79*, 176–185.
- (18) Van Gool, F.; Galli, M.; Gueydan, C.; Kruys, V.; Prevot, P. P.; Bedalov, A.; Mostoslavsky, R.; Alt, F. W.; De Smedt, T.; Leo, O. Intracellular NAD levels regulate tumor necrosis factor protein synthesis in a sirtuin-dependent manner. *Nat. Med.* **2009**, *15* (2), 206–210.
- (19) Jiang, H.; Khan, S.; Wang, Y.; Charron, G.; He, B.; Sebastian, C.; Du, J.; Kim, R.; Ge, E.; Mostoslavsky, R.; Hang, H. C.; Hao, Q.; Lin, H. SIRT6 regulates TNF- α secretion through hydrolysis of long-chain fatty acyl lysine. *Nature* **2013**, *496* (7443), 110–113.
- (20) Curry, A. M.; White, D. S.; Donu, D.; Cen, Y. Human Sirtuin Regulators: The "Success" Stories. *Front. Physiol.* **2021**, *12*, 752117.
- (21) Dang, W. The controversial world of sirtuins. *Drug Discov. Today Technol.* **2014**, *12*, e9–e17.
- (22) Lee, Y. T.; Tan, Y. J.; Mok, P. Y.; Subramaniam, A. V.; Oon, C. E. Chapter 9—The bifunctional roles of sirtuins and their therapeutic potential in cancer. In *Sirtuin Biology in Cancer and Metabolic Disease*; Maiese, K., Ed.; Academic Press, 2021; pp 153–177.
- (23) Du, J.; Jiang, H.; Lin, H. Investigating the ADP-ribosyltransferase activity of sirtuins with NAD analogues and 32P-NAD. *Biochemistry* **2009**, *48* (13), 2878–2890.
- (24) Colak, G.; Xie, Z.; Zhu, A. Y.; Dai, L.; Lu, Z.; Zhang, Y.; Wan, X.; Chen, Y.; Cha, Y. H.; Lin, H.; Zhao, Y.; Tan, M. Identification of lysine succinylation substrates and the succinylation regulatory enzyme CobB in *Escherichia coli*. *Mol. Cell. Proteomics* **2013**, *12* (12), 3509–3520.
- (25) Ravi, V.; Jain, A.; Khan, D.; Ahamed, F.; Mishra, S.; Giri, M.; Inbaraj, M.; Krishna, S.; Sarikhani, M.; Maity, S.; Kumar, S.; Shah, R. A.; Dave, P.; Pandit, A. S.; Rajendran, R.; Desingu, P. A.; Varshney, U.; Das, S.; Kolthur-Seetharam, U.; Rajakumari, S.; Singh, M.; Sundaresan, N. R. SIRT6 transcriptionally regulates global protein synthesis through transcription factor Sp1 independent of its deacetylase activity. *Nucleic Acids Res.* **2019**, *47* (17), 9115–9131.
- (26) Graham, E.; Rymarchyk, S.; Wood, M.; Cen, Y. Development of Activity-Based Chemical Probes for Human Sirtuins. *ACS Chem. Biol.* **2018**, *13* (3), 782–792.
- (27) Wood, M.; Rymarchyk, S.; Zheng, S.; Cen, Y. Trichostatin A inhibits deacetylation of histone H3 and p53 by SIRT6. *Arch. Biochem. Biophys.* **2018**, *638*, 8–17.
- (28) Liu, W. H.; Zheng, J.; Feldman, J. L.; Klein, M. A.; Kuznetsov, V. I.; Peterson, C. L.; Griffin, P. R.; Denu, J. M. Multivalent interactions drive nucleosome binding and efficient chromatin deacetylation by SIRT6. *Nat. Commun.* **2020**, *11* (1), 5244.
- (29) Meng, F.; Qian, M.; Peng, B.; Peng, L.; Wang, X.; Zheng, K.; Liu, Z.; Tang, X.; Zhang, S.; Sun, S.; Cao, X.; Pang, Q.; Zhao, B.; Ma, W.; Songyang, Z.; Xu, B.; Zhu, W. G.; Xu, X.; Liu, B. Synergy between SIRT1 and SIRT6 helps recognize DNA breaks and potentiates the DNA damage response and repair in humans and mice. *Elife* **2020**, *9*, No. e55828.
- (30) Gil, R.; Barth, S.; Kanfi, Y.; Cohen, H. Y. SIRT6 exhibits nucleosome-dependent deacetylase activity. *Nucleic Acids Res.* **2013**, *41* (18), 8537–8545.
- (31) Wang, Z. A.; Markert, J. W.; Whedon, S. D.; Yapa Abeywardana, M.; Lee, K.; Jiang, H.; Suarez, C.; Lin, H.; Farnung, L.; Cole, P. A. Structural Basis of Sirtuin 6-Catalyzed Nucleosome Deacetylation. *J. Am. Chem. Soc.* **2023**, *145* (12), 6811–6822.
- (32) Smirnova, E.; Bignon, E.; Schultz, P.; Papai, G.; Ben-Shem, A. Binding to nucleosome poises SIRT6 for histone H3 de-acetylation. *bioRxiv* **2023**, DOI: 10.1101/2023.03.20.533444.
- (33) Van Meter, M.; Simon, M.; Tomblin, G.; May, A.; Morello, T. D.; Hubbard, B. P.; Bredbenner, K.; Park, R.; Sinclair, D. A.; Bohr, V. A.; Gorbunova, V.; Seluanov, A. JNK Phosphorylates SIRT6 to Stimulate DNA Double-Strand Break Repair in Response to Oxidative Stress by Recruiting PARP1 to DNA Breaks. *Cell Rep.* **2016**, *16* (10), 2641–2650.
- (34) Mao, Z.; Hine, C.; Tian, X.; Van Meter, M.; Au, M.; Vaidya, A.; Seluanov, A.; Gorbunova, V. SIRT6 promotes DNA repair under stress by activating PARP1. *Science* **2011**, *332* (6036), 1443–1446.
- (35) Toiber, D.; Erdel, F.; Bouazoune, K.; Silberman, D. M.; Zhong, L.; Mulligan, P.; Sebastian, C.; Cosentino, C.; Martinez-Pastor, B.; Giacosa, S.; D'Urso, A.; Naar, A. M.; Kingston, R.; Rippe, K.; Mostoslavsky, R. SIRT6 recruits SNF2H to DNA break sites, preventing genomic instability through chromatin remodeling. *Mol. Cell* **2013**, *51* (4), 454–468.
- (36) Tjeertes, J. V.; Miller, K. M.; Jackson, S. P. Screen for DNA-damage-responsive histone modifications identifies H3K9Ac and H3K56Ac in human cells. *EMBO J.* **2009**, *28* (13), 1878–1889.
- (37) McCord, R. A.; Michishita, E.; Hong, T.; Berber, E.; Boxer, L. D.; Kusumoto, R.; Guan, S.; Shi, X.; Gozani, O.; Burlingame, A. L.; Bohr, V. A.; Chua, K. F. SIRT6 stabilizes DNA-dependent protein kinase at chromatin for DNA double-strand break repair. *Aging (Albany NY)* **2009**, *1* (1), 109–121.
- (38) Van Meter, M.; Mao, Z.; Gorbunova, V.; Seluanov, A. Repairing split ends: SIRT6, mono-ADP ribosylation and DNA repair. *Aging (Albany NY)* **2011**, *3* (9), 829–835.
- (39) Hwang, S.; Gou, Z.; Kuznetsov, I. B. DP-Bind: a web server for sequence-based prediction of DNA-binding residues in DNA-binding proteins. *Bioinformatics* **2007**, *23* (5), 634–636.
- (40) Kuznetsov, I. B.; Gou, Z.; Li, R.; Hwang, S. Using evolutionary and structural information to predict DNA-binding sites on DNA-binding proteins. *Proteins* **2006**, *64* (1), 19–27.
- (41) Pan, P. W.; Feldman, J. L.; Devries, M. K.; Dong, A.; Edwards, A. M.; Denu, J. M. Structure and biochemical functions of SIRT6. *J. Biol. Chem.* **2011**, *286* (16), 14575–14587.
- (42) Jumper, J.; Evans, R.; Pritzel, A.; Green, T.; Figurnov, M.; Ronneberger, O.; Tunyasuvunakool, K.; Bates, R.; Zidek, A.; Potapenko, A.; Bridgland, A.; Meyer, C.; Kohli, S. A. A.; Ballard, A. J.; Cowie, A.; Romera-Paredes, B.; Nikolov, S.; Jain, R.; Adler, J.; Back, T.; Petersen, S.; Reiman, D.; Clancy, E.; Zielinski, M.; Steinegger, M.; Pacholska, M.; Berghammer, T.; Bodenstein, S.; Silver, D.; Vinyals, O.; Senior, A. W.; Kavukcuoglu, K.; Kohli, P.; Hassabis, D. Highly accurate protein structure prediction with AlphaFold. *Nature* **2021**, *596* (7873), 583–589.
- (43) Varadi, M.; Anyango, S.; Deshpande, M.; Nair, S.; Natassia, C.; Yordanova, G.; Yuan, D.; Stroe, O.; Wood, G.; Laydon, A.; Zidek, A.; Green, T.; Tunyasuvunakool, K.; Petersen, S.; Jumper, J.; Clancy, E.; Green, R.; Vora, A.; Lutfi, M.; Figurnov, M.; Cowie, A.; Hobbs, N.; Kohli, P.; Kleywegt, G.; Birney, E.; Hassabis, D.; Velankar, S. AlphaFold Protein Structure Database: massively expanding the structural coverage of protein-sequence space with high-accuracy models. *Nucleic Acids Res.* **2022**, *50* (D1), D439–D444.
- (44) Feldman, J. L.; Baeza, J.; Denu, J. M. Activation of the protein deacetylase SIRT6 by long-chain fatty acids and widespread deacetylation by mammalian sirtuins. *J. Biol. Chem.* **2013**, *288* (43), 31350–31356.
- (45) Cui, X.; Yao, L.; Yang, X.; Gao, Y.; Fang, F.; Zhang, J.; Wang, Q.; Chang, Y. SIRT6 regulates metabolic homeostasis in skeletal muscle through activation of AMPK. *Am. J. Physiol. Endocrinol. Metabol.* **2017**, *313* (4), E493–E505.
- (46) Charron, G.; Zhang, M. M.; Yount, J. S.; Wilson, J.; Raghavan, A. S.; Shamir, E.; Hang, H. C. Robust fluorescent detection of protein

fatty-acylation with chemical reporters. *J. Am. Chem. Soc.* **2009**, *131* (13), 4967–4975.

(47) Yang, B.; Zwaans, B. M.; Eckersdorff, M.; Lombard, D. B. The sirtuin SIRT6 deacetylates H3 K56Ac in vivo to promote genomic stability. *Cell Cycle* **2009**, *8* (16), 2662–2663.

(48) Tennen, R. I.; Bua, D. J.; Wright, W. E.; Chua, K. F. SIRT6 is required for maintenance of telomere position effect in human cells. *Nat. Commun.* **2011**, *2*, 433.

(49) Zhong, L.; D'Urso, A.; Toiber, D.; Sebastian, C.; Henry, R. E.; Vadysirisack, D. D.; Guimaraes, A.; Marinelli, B.; Wikstrom, J. D.; Nir, T.; Clish, C. B.; Vaitheesvaran, B.; Iliopoulos, O.; Kurland, I.; Dor, Y.; Weissleder, R.; Shirihai, O. S.; Ellisen, L. W.; Espinosa, J. M.; Mostoslavsky, R. The Histone Deacetylase Sirt6 Regulates Glucose Homeostasis via Hif1 α . *Cell* **2010**, *140* (2), 280–293.

(50) D'Onofrio, N.; Servillo, L.; Balestrieri, M. L. SIRT1 and SIRT6 Signaling Pathways in Cardiovascular Disease Protection. *Antioxid. Redox Signaling* **2018**, *28* (8), 711–732.

(51) Kuang, J.; Chen, L.; Tang, Q.; Zhang, J.; Li, Y.; He, J. The Role of Sirt6 in Obesity and Diabetes. *Front. Physiol.* **2018**, *9*, 135.

(52) Kugel, S.; Mostoslavsky, R. Chromatin and beyond: the multitasking roles for SIRT6. *Trends Biochem. Sci.* **2014**, *39* (2), 72–81.

(53) Van Meter, M.; Gorbunova, V.; Seluanov, A. SIRT6: a promising target for cancer prevention and therapy. *Adv. Exp. Med. Biol.* **2014**, *818*, 181–196.

(54) Kawahara, T. L.; Michishita, E.; Adler, A. S.; Damian, M.; Berber, E.; Lin, M.; McCord, R. A.; Ongaigui, K. C.; Boxer, L. D.; Chang, H. Y.; Chua, K. F. SIRT6 Links Histone H3 Lysine 9 Deacetylation to NF- κ B-Dependent Gene Expression and Organismal Life Span. *Cell* **2009**, *136* (1), 62–74.